Precision and fast wavelength tuning of a dynamically phase-locked widely-tunable laser

Kenji Numata,[1,2,*] Jeffrey R. Chen,[2] and Stewart T. Wu[2]

[1]*Department of Astronomy, University of Maryland, College Park, Maryland 20742, USA*
[2]*NASA Goddard Space Flight Center, Greenbelt, Maryland 20771, USA*
[*]*kenji.numata@nasa.gov*

Abstract: We report a precision and fast wavelength tuning technique demonstrated for a digital-supermode distributed Bragg reflector laser. The laser was dynamically offset-locked to a frequency-stabilized master laser using an optical phase-locked loop, enabling precision fast tuning to and from any frequencies within a ~40-GHz tuning range. The offset frequency noise was suppressed to the statically offset-locked level in less than ~40 μs upon each frequency switch, allowing the laser to retain the absolute frequency stability of the master laser. This technique satisfies stringent requirements for gas sensing lidars and enables other applications that require such well-controlled precision fast tuning.

OCIS codes: (140.5960) Semiconductor lasers; (140.3600) Lasers, tunable; (010.3640) Lidar; (140.3425) Laser stabilization.

References and links

1. A. J. Ward, D. J. Robbins, G. Busico, E. Barton, L. Ponnampalam, J. P. Duck, N. D. Whitbread, P. J. Williams, D. C. J. Reid, A. C. Carter, and M. J. Wale, "Widely tunable DS-DBR laser with monolithically integrated SOA: design and performance," IEEE J. Sel. Top. Quantum Electron. **11**(1), 149–156 (2005).
2. Y. A. Akulova, G. A. Fish, Ping-Chiek Koh, C. L. Schow, P. Kozodoy, A. P. Dahl, S. Nakagawa, M. C. Larson, M. P. Mack, T. A. Strand, C. W. Coldren, E. Hegblom, S. K. Penniman, T. Wipiejewski, and L. A. Coldren, "Widely tunable electroabsorption-modulated sampled-grating DBR laser transmitters," IEEE J. Sel. Top. Quantum Electron. **8**(6), 1349–1357 (2002).
3. M. Mestre, J. M. Fabrega, J. A. Lazaro, V. Polo, A. Djupsjobacka, M. Forzati, P. Rigole, and J. Prat, "Tuning characteristics and switching speed of a modulated grating Y structure laser for wavelength routed PONs," in Access Networks and In-house Communications, OSA Technical Digest (CD) (Optical Society of America, 2010), paper AThC2.
4. M. Oberg, S. Nilsson, K. Streubel, J. Wallin, L. Backbom, and T. Klinga, "74 nm wavelength tuning range of an InGaAsP/InP vertical grating assisted codirectional coupler laser with rear sampled grating reflector," IEEE Photon. Technol. Lett. **5**(7), 735–737 (1993).
5. J. Buus and E. J. Murphy, "Tunable lasers in optical networks," J. Lightwave Technol. **24**(1), 5–11 (2006).
6. R. Phelan, M. Lynch, J. F. Donegan, and V. Weldon, "Simultaneous multispecies gas sensing by use of a sampled grating distributed Bragg reflector and modulated grating Y laser diode," Appl. Opt. **44**(27), 5824–5831 (2005).
7. B. Puttnam, M. Dueser, B. Thomsen, P. Bayvel, A. Bianciotto, R. Gaudino, G. Busico, L. Ponnampalam, D. Robbins, and N. Whitbread, "Burst mode operation of a DS-DBR widely tunable laser for wavelength agile system applications," in Proceedings of Optical Fiber Communication Conference (OFC) (Optical Society of America, 2006), Paper OW186.
8. J. E. Simsarian, M. C. Larson, H. E. Garrett, H. Xu, and T. A. Strand, "Less than 5-ns wavelength switching with an SG-DBR laser," IEEE Photon. Technol. Lett. **18**(4), 565–567 (2006).
9. Space studies board, National research council, *Earth Science and Applications from Space: National Imperatives for the Next Decade and Beyond* (National Academies Press, 2007), Chap. 4.
10. J. B. Abshire, H. Riris, G. Allan, X. Sun, S. R. Kawa, J. Mao, M. Stephen, E. Wilson, and M. A. Krainak, "Laser sounder for global measurement of CO_2 concentrations in the troposphere from space," in Laser Applications to Chemical, Security and Environmental Analysis of OSA Technical Digest Series (CD) (Optical Society of America, 2008), paper LMA4.
11. J. Mao and S. R. Kawa, "Sensitivity studies for space-based measurement of atmospheric total column carbon dioxide by reflected sunlight," Appl. Opt. **43**(4), 914–927 (2004).
12. S. R. Kawa, J. Mao, J. B. Abshire, G. J. Collatz, X. Sun, and C. J. Weaver, "Simulation studies for a space-based CO_2 lidar mission," Tellus, Ser. B, Chem. Phys. Meteorol. **62**(5), 759–769 (2010).
13. J. R. Chen, K. Numata, and S. T. Wu, "Error reduction methods for integrated path differential absorption lidar measurements," submitted to Opt. Express (2012).

#167248 - $15.00 USD Received 23 Apr 2012; revised 31 May 2012; accepted 1 Jun 2012; published 12 Jun 2012

14. K. Numata, J. R. Chen, S. T. Wu, J. B. Abshire, and M. A. Krainak, "Frequency stabilization of distributed-feedback laser diodes at 1572 nm for lidar measurements of atmospheric carbon dioxide," Appl. Opt. **50**(7), 1047–1056 (2011).
15. L. Ponnampalam, D. J. Robbins, A. J. Ward, N. D. Whitbread, J. P. Duck, G. Busico, and D. J. Bazley, "Equivalent performance in C- and L-bands of digital supermode distributed Bragg reflector lasers," IEEE J. Quantum Electron. **43**(9), 798–803 (2007).
16. C. J. Erickson, M. Van Zijll, G. Doermann, and D. S. Durfee, "An ultrahigh stability, low-noise laser current driver with digital control," Rev. Sci. Instrum. **79**(7), 073107 (2008).
17. P. Correc, O. Girard, and I. F. de Faria, Jr., "On the thermal contribution to the FM response of DFB lasers: theory and experiment," IEEE J. Quantum Electron. **30**(11), 2485–2490 (1994).
18. Analog Devices, AD9858 datasheet, *http://www.analog.com/static/imported-files/data_sheets/AD9858.pdf*.
19. J. Ye and J. L. Hall, "Optical phase locking in the microradian domain: potential applications to NASA spaceborne optical measurements," Opt. Lett. **24**(24), 1838–1840 (1999).
20. J. I. Thorpe, K. Numata, and J. Livas, "Laser frequency stabilization and control through offset sideband locking to optical cavities," Opt. Express **16**(20), 15980–15990 (2008).
21. L. Consolino, G. Giusfredi, P. De Natale, M. Inguscio, and P. Cancio, "Optical frequency comb assisted laser system for multiplex precision spectroscopy," Opt. Express **19**(4), 3155–3162 (2011).
22. A. S. Olesen, A. T. Pedersen, and K. Rottwitt, "Frequency stepped pulse train modulated wind sensing lidar," Proc. SPIE **8159**, 81590O, 81590O-8 (2011).

1. Introduction

Various widely-tunable monolithic semiconductor diode lasers have been developed for telecom applications. They include a digital-supermode distributed-Bragg-reflector (DS-DBR) laser [1], a sampled-grating DBR (SG-DBR) laser [2], and other types of lasers (see, for example [3, 4]). These single-mode lasers can be tuned over tens of nanometers in wavelength. Fast wavelength switching of such lasers has been sought for dynamic wavelength provisioning in future optical networks [5]. They have found additional spectroscopic applications for multispecies gas sensing [6]. The wavelength of such lasers can be rapidly switched and locked within ~12 μs for a step size over 30 nm [7, 8]. Limited by the coarse frequency locking techniques employed in such demonstrations, the uncertainty of the locked laser frequency was as large as a few GHz, which still satisfies current telecom requirements. In this paper, we report a tuning technique to drastically improve the frequency precision while retaining the fast tuning speed of such widely tunable lasers.

The work presented here is motivated by the Active Sensing of CO_2 Emissions over Nights, Days, and Seasons (ASCENDS) mission [9] which is planned by NASA to measure the global distribution of carbon dioxide (CO_2) mixing ratios from an Earth-orbiting satellite. This mission has set unprecedented targets for precision that require much better laser frequency precision than most telecom applications. A candidate lidar for ASCENDS being developed at NASA Goddard uses a nadir-viewing, integrated path differential absorption lidar technique to scan a single atmospheric CO_2 absorption line [10, 11] at 1572.335 nm. A pulsed laser rapidly steps through multiple fixed wavelengths across the CO_2 line [10]. The 1-μs wide laser pulses are ~100 μs apart and the wavelength is switched pulse by pulse. The differential absorption optical depth and the corresponding column number density of CO_2 can be determined from post-detection analysis [12]. The laser frequency fluctuation causes a variation in measured CO_2 transmittance, resulting in an uncertainty in the column number density estimation. The error caused by the frequency uncertainty needs to be a small fraction of the measurement error budget. As a result, the effective frequency noise (standard deviation) needs to be < 0.23 MHz for the ASCENDS mission [13].

Using the laser tuning technique summarized here, such a frequency-stepped pulse train has been generated from a single fast tunable slave laser. As conceptually illustrated in Fig. 1, the tunable slave DS-DBR laser was dynamically offset-locked to a frequency-stabilized master (reference) laser using a fast tunable optical phase-locked loop (OPLL) technique. This enabled precision fast tuning of the slave laser to and from any frequencies within a ~40 GHz (0.33 nm) tuning range. In less than ~40 μs upon each frequency switch, the frequency noise of the slave laser was suppressed to the same level as achieved when the same laser was statically offset-locked. The master distributed-feedback laser diode (DFB-LD) is locked to the line center (ν_0 in Fig. 1) of the CO_2 line by a frequency-modulation technique [14]. The

#167248 - $15.00 USD Received 23 Apr 2012; revised 31 May 2012; accepted 1 Jun 2012; published 12 Jun 2012

continuous wave (CW) output from the slave DS-DBR laser is carved into the frequency-stepped pulse train (cycling from ν_1 to ν_8) by a chirp-free Mach-Zehnder modulator (MZM). For space-borne CO_2 remote sensing, this pulsed seed laser output needs to be subsequently amplified by laser amplifiers to achieve the pulse energy level required for the measurements. In order to reduce statistical errors from various sources, the detected pulse energies for each wavelength are averaged across multiple laser pulses in deriving the differential absorption optical depth [13]. The demonstrated tuning range, switching time, and frequency stability satisfies the ASCENDS requirements. The dynamic offset-locking technique presented here can also be applied to other applications that require such well-controlled fast tuning.

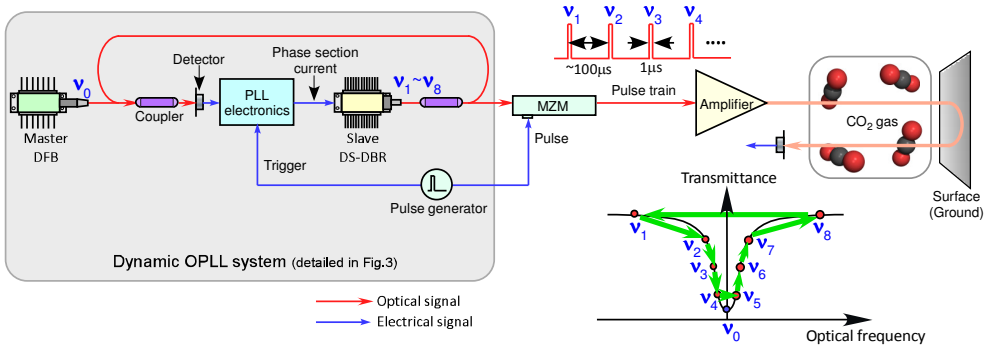

Fig. 1. Concept of the precision fast laser tuning technique and its application for CO_2 remote sensing. The DS-DBR laser is dynamically offset-locked to the master DFB-LD using a dynamic OPLL. The frequency-stepped pulse train is formed by external modulation through the MZM and subsequent amplification. The amplified pulse train is used to repeatedly measure at multiple points across the CO_2 absorption line. PLL: phase-locked loop.

2. Experimental setup

The present precision and fast tuning technique is enabled by the fast tuning response of the DS-DBR laser through its phase section and the fast tunable OPLL, as detailed below in Sections 2.1 and 2.2 respectively.

2.1DS-DBR laser source

A DS-DBR laser, lifted from an integrated tunable laser assembly (TL5000DLJ, Oclaro Inc.), was used as the slave laser in the OPLL. The laser has an 8-contact chirped front grating, a rear phase-grating, a phase section for fine tuning, and a gain section. It also employs a monolithically integrated semiconductor optical amplifier section in front of the laser to boost the output power to ~10 dBm [15]. The free-running laser frequency noise was drastically reduced by using low-noise current drivers [16] to provide constant currents. By adjusting currents to the phase, front, and rear mirror sections, the center wavelength of this laser can be tuned over the L-band (1568~1647 nm). In this work, the center wavelength was set at 1572.335 nm by current driving one contact of the front grating while grounding all other seven contacts. The tuning signal was applied to the phase section through a 20 MHz modulation port of the current driver that also provides an additive constant bias current.

The fast tuning speed of the DS-DBR laser is enabled by the non-thermal tuning mechanism of its phase, front and rear grating sections. The effective refractive indices of these sections are shifted through the carrier injection by the tuning currents. Although a DFB-LD exhibits lower frequency noise and was thus chosen as the master laser, its tuning speed is much lower because the tuning arises mainly from the slower heating effect of the injection current [17]. This is illustrated in Fig. 2 where measured frequency shifts of the DS-DBR laser (a) and the DFB-LD (b) are plotted as functions of a tuning current ramping in a triangular waveform. The DS-DBR laser was tuned by changing its phase section current and the DFB-LD was tuned by ramping its gain section current. Identical low-noise current

#167248 - $15.00 USD Received 23 Apr 2012; revised 31 May 2012; accepted 1 Jun 2012; published 12 Jun 2012

drivers were used to drive both lasers. The tuning curve of the DS-DBR laser is essentially independent of the modulation frequency and tuning direction. In contrast, the DFB-LD exhibits large tuning hysteresis and decaying tuning efficiency with the modulation frequency, making it unsuitable for fast frequency tuning and control. The DS-DBR laser was chosen over a SG-DBR laser because of the lower frequency noise and wider phase section tuning range (~40 GHz) measured in the former.

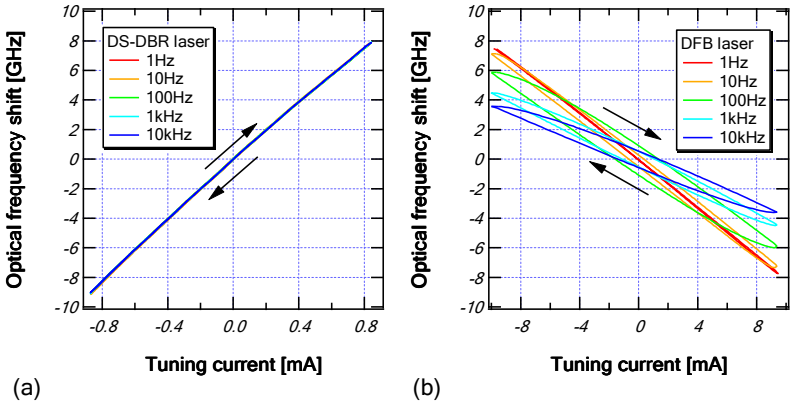

Fig. 2. The optical frequency shifts of the DS-DBR laser (a) and the DFB-LD (b) as functions of a tuning current ramping in a triangular waveform.

2.2 OPLL electronics

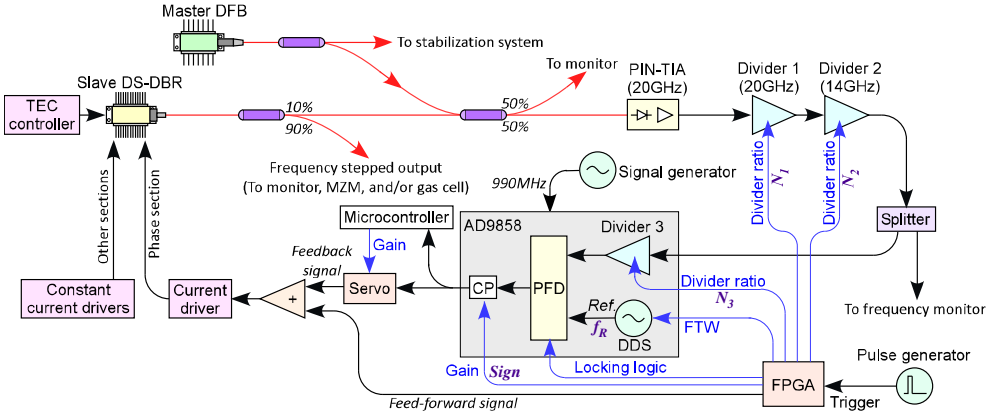

Fig. 3. OPLL experimental setup. TEC, thermoelectric cooler.

Figure 3 shows the details of our dynamic OPLL system. The beatnote between the slave DS-DBR laser and the master DFB-LD was detected by a 20 GHz receiver that consists of a PIN photodiode followed by an integrated transimpedance amplifier (TIA) (DSC-R401HG-39-FC/APC-K-1, Discovery Semiconductors, Inc.). The beatnote was frequency-divided by a programmable factor N and dynamically phase-locked to a changing RF reference signal generated by a direct digital synthesizer (DDS). Fast frequency switching was achieved by using a feed-forward tuning signal. Subsequent phase-lock was acquired rapidly by employing a fast-locking logic. A digital phase/frequency detector (PFD) detects the phase difference between the divided beatnote and the RF reference signal, and drives a charge pump (CP) to generate an error signal proportional to this phase difference. A servo circuit turned the error signal into a feedback signal that was added to the feed-forward signal. The sum was fed to the current driver for the phase section to tune the slave laser. The PLL brings

#167248 - $15.00 USD Received 23 Apr 2012; revised 31 May 2012; accepted 1 Jun 2012; published 12 Jun 2012

the offset frequency to its target $Sign \cdot N \cdot f_R$, where f_R is the reference frequency and *Sign* is either + or -. The feed-forward signal alone forces the laser frequency to track the moving target closely, leaving a small residual offset frequency error. The residual phase error is suppressed by the PLL.

A commercial IC chip (AD9858, Analog Devices, Inc.) was used to provide the PFD, CP, and DDS functions [18]. The open-loop unity-gain bandwidth of the final loop was measured to be ~100 kHz. The base clock for this IC was 990 MHz provided by an external signal generator. Three frequency dividers, divider 1 and 2 (UXD20PE and UXN14M9PE, Centellax, Inc.) and divider 3 (integrated in AD9858), were used to divide the beatnote frequency to below the maximum frequency (150 MHz) of the PFD. The total frequency-dividing factor N is the product of the three divider ratios, N_1, N_2, and N_3. A field programmable gate array (FPGA) card was used to generate the feed-forward signal and to dynamically control loop parameters, such as the gain and sign for the CP current, DDS frequency, and dividing factors of the three frequency dividers. A microcontroller was also used to control the gain and switches in the servo circuit. The FPGA waited on a triggering pulse from the pulse generator to start each frequency switch.

2.3 Frequency plan

Table 1. Target Offset Frequencies, Their Corresponding Frequency Divider Settings, and Reference DDS Frequencies for the Eight Wavelength Points

Offset frequency (GHz)	Divider 1 ratio N_1	Divider 2 ratio N_2	Frequency monitor (MHz)	Divider 3 ratio N_3	DDS frequency f_R (MHz)
± 15.6	8	12	162.5	2	81.25
± 1.70	1	8	212.5	2	106.25
± 1.08	1	8	135	2	67.5
± 0.50	1	8	62.5	1	62.5

The slave DS-DBR laser can be fast tuned to and from any frequencies around the master laser frequency within ± 20 GHz. To do this, the three factors, *Sign*, N, and f_R, need to be changed rapidly. Table 1 shows an example set of settings for the frequency dividers and the DDS for target offset frequencies ± 15.6 GHz, ± 1.70 GHz, ± 1.08 GHz, and ± 0.50 GHz. The DDS frequency was set by issuing a frequency tuning word (FTW) from the FPGA. Polarity (*Sign*) switching of the offset frequency was achieved by changing the sign of the CP current. The target offset frequency and the feed-forward signal were simultaneously switched without transitional sweeping. The parallel port of AD9858 allows FTW and other control commands to be transmitted at up to 125 MB/s. Limited by the 40 MHz clock rate of the FPGA, it took ~1 μs to change all three factors in $Sign \cdot N \cdot f_R$ and the CP gain.

3. Experimental results

3.1 Performance of statically offset-locked laser

The performance of the OPLL was first evaluated at a fixed offset frequency. The stability of the offset frequency was measured from the beatnote between the slave laser and its master laser. The stability of the slave laser's absolute frequency was measured from the beatnote between this slave and an independent replica of the master laser that was also frequency-stabilized to the CO_2 line.

#167248 - $15.00 USD Received 23 Apr 2012; revised 31 May 2012; accepted 1 Jun 2012; published 12 Jun 2012

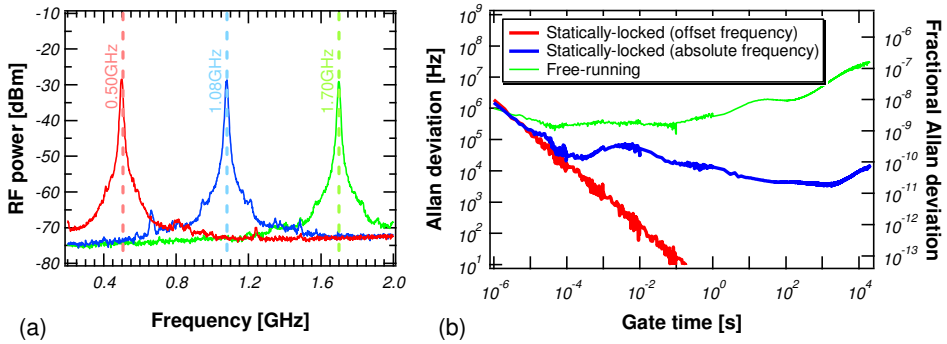

Fig. 4. (a) The RF spectra of the master-slave beatnote for the three offset locking points. The resolution bandwidth of the RF spectrum analyzer was 3 MHz. (b) Allan deviations of the offset and absolute frequencies of the slave laser when statically-locked, and of the absolute frequency of the slave laser when unlocked.

Figure 4 (a) shows the short-term RF spectra of the master-slave beatnote measured with a RF spectrum analyzer for the three offset frequencies. At each offset frequency, the full width at half maximum of the spectral peak was measured to be ~30 MHz. Since the linewidth of the master laser was much narrower (~2 MHz), the linewidth of the DS-DBR laser was estimated to be ~30 MHz, arising from its unsuppressed fast frequency noise components. Figure 4 (b) shows Allan deviations of the offset and absolute frequencies of the statically-locked DS-DBR laser (at an offset frequency of + 1.08 GHz), in comparison to the absolute-frequency Allan deviation of the slave laser when it was free-running. Since the offset frequency drifts were suppressed by the OPLL, the deviation of the offset frequency kept decreasing as the gate (averaging) time was increased. In other words, the phase locking essentially does not contribute to the long term frequency drifts of the slave laser. As a result, the absolute frequency Allan deviation of the statically-locked slave laser essentially represented that of the master laser when the gate time was longer than 10 μs (which is the inverse of the 100-kHz control bandwidth). Compared to the free-running case, the OPLL suppressed the long-term frequency drifts of the slave laser by a factor of ~1000, reducing the fractional Allan deviation to below 10^{-10} when the gate time was over 1 s. This long-term absolute stability of the slave laser is limited by that of the master laser [14], not limited by the present phase-locking technique.

3.2 Performance of dynamically offset-locked laser

With the setup shown in Fig. 3, we successfully achieved the desired precision for the fast laser frequency stepping. The magnitude of the offset frequency was monitored at the frequency monitor point (after divider 1 and 2). To monitor the polarity of the offset frequency and the absolute frequency noise of the slave DS-DBR laser, we also measured the beatnote between this slave laser and another slave DFB-LD offset locked to the other (independent) reference DFB-LD. A fast frequency counter (HP 5371A, Agilent Technologies, Inc.) was used to measure the frequencies of the divided beatnotes and the electronic reference signal with a 1-μs gate time.

Figure 5 plots the time sequences of the measured offset frequency and relevant signals. The DDS frequency, frequency dividing ratios, CP current polarity and magnitude, and the feed-forward signal were stepped synchronously. The feedback signal automatically compensated for the imperfection in the feed-forward signal in order to acquire and maintain the phase-lock. There was no loss of lock over several days of operation.

Two closer views of the optical frequency changes are shown in Fig. 6, for the best case (a) with a + 0.58 GHz jump and no polarity change, and the worst case (b) with the largest jump (−31.2 GHz step) and polarity change. For the best case, the offset frequency settled down to the target frequency (+ 1.08 GHz) within ~5 μs. For the worst case, the offset

#167248 - $15.00 USD Received 23 Apr 2012; revised 31 May 2012; accepted 1 Jun 2012; published 12 Jun 2012

frequency settled down to the target frequency (−15.6 GHz) in less than 40 µs. Once settled, the standard deviation of the offset frequency was ~1 MHz at a 1 µs averaging time. Without the feedback signal (open loop), the offset frequency missed the target with much larger errors.

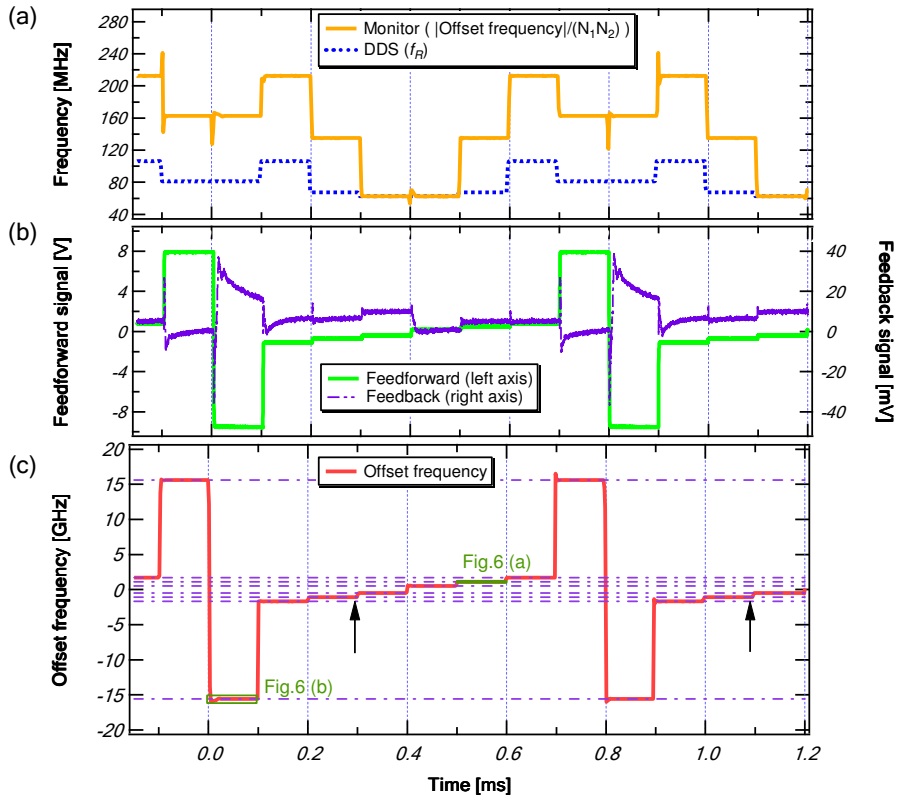

Fig. 5. Measured offset frequency and relevant signals as functions of time. (a) Divided beatnote measured after divider 1 and 2, and the reference DDS frequency. (b) The feed-forward voltage (left axis) and the feedback voltage (right axis). (c) The offset frequency between the slave and the master lasers. The dashed horizontal lines indicate target offset frequencies. Closer views of the two frequency steps (corresponding to the two green boxes) are shown in Fig. 6. The arrows indicate time points when the optical frequency for this step was periodically measured for statistical evaluation, as shown in Fig. 7.

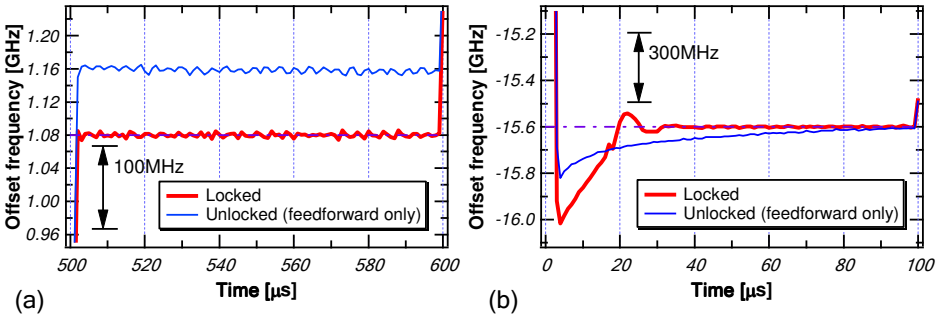

Fig. 6. Closer view of two frequency steps. (a) Easiest step with + 0.58 GHz jump and no polarity change. (b) Hardest step with −31.2 GHz jump and polarity change. The dashed lines indicate target offset frequencies (+ 1.08 GHz and −15.6 GHz, respectively).

#167248 - $15.00 USD Received 23 Apr 2012; revised 31 May 2012; accepted 1 Jun 2012; published 12 Jun 2012

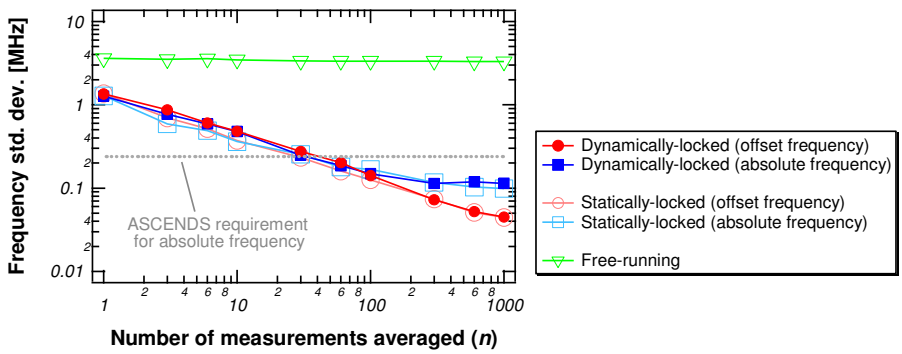

Fig. 7. Relationships between the standard deviations of averaged laser offset and absolute frequencies, and the number of measurements (pulses) being averaged. The gate time used for each measurement is 1 μs.

In order to evaluate the laser frequency stability statistically, each offset frequency and corresponding absolute frequency of the slave laser were measured periodically within a 1-μs gate time and averaged across multiple measurements. Then the standard deviation of the averaged frequencies was calculated. (Rather than using Allan deviation where the gate time is varied and the longer-timescale drifts are excluded, we included the drifts by using the standard deviation for a fixed gate time to evaluate the frequency stability.) Each measurement was taken at the end of the frequency step when the laser pulse is to be carved for CO_2 measurements (as indicated by the arrows in Fig. 5 for an offset frequency of −1.08 GHz). The standard deviations for this frequency step are plotted in Fig. 7 as functions of n, the number of measurements being averaged. These curves are representative for all frequency steps. When the laser was dynamically locked, both standard deviation curves were found to be identical to those obtained when the same laser was statically locked. This indicates that dynamic locking does not degrade the frequency noise suppression performance. The standard deviation of the averaged offset frequency was found to be proportional to $1/\sqrt{n}$, indicating that the offset frequency errors were uncorrelated among the measurements. This allows the offset frequency noise to be averaged down to a negligible level so that the slave laser retains the frequency stability of the master laser. Due to slow master-laser frequency drifts, the standard deviation of the averaged absolute frequency settled to ~0.1 MHz for $n > 300$. The absolute frequency stability requirement for ASCENDS (0.23 MHz [13]) was met with $n > 60$. In contrast, such averaging does not reduce the frequency noise of the slave laser when it is free running, due to its dominant long-term frequency drifts.

3.3 Demonstration of gas absorption measurement

Precision and fast absorption measurement of the CO_2 line was demonstrated by passing the DS-DBR laser output through an 18-m gas cell filled with 100-Torr CO_2. Figure 8(a) shows the measured transmittance vs. time while the laser frequency was stepped with and without the pulse modulation by the MZM. By synchronously triggering the FPGA, the frequency switching was synchronized to the pulse carving occurring at the end of each frequency step. Biased at a null point, the MZM's on/off extinction ratio (> 40 dB) exhibited little degradation (hence little optical leakage at the off state) when the laser wavelength was rapidly switched within a bandwidth of a few nanometers. The CO_2 transmittance spectrum was also measured by continuously scanning the same laser and carefully calibrating the optical frequency from the beatnote between the slave and master lasers. As shown in Fig. 8 (b), the transmittance measured in the frequency stepped mode (solid circles) agreed well with that measured continuously (solid line), confirming the accuracy of the stepped frequency scan.

#167248 - $15.00 USD Received 23 Apr 2012; revised 31 May 2012; accepted 1 Jun 2012; published 12 Jun 2012

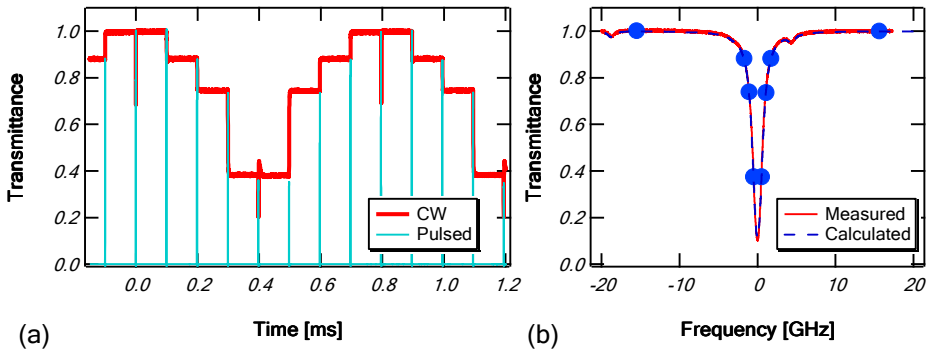

Fig. 8. Measured transmittance of CO_2 in a gas cell using the scanning DS-DBR laser. (a) Transmittance vs. time measured in frequency-stepped mode with and without the pulse modulation. (b) Transmittance spectra measured by continuously scanning the same laser (solid line) and by stepping the frequency (solid circle). The calculated transmittance (dashed blue) is also plotted for comparison.

4. Discussions

4.1 Comparison to other methods

Among various PLL techniques, our PFD-based scheme appears to be most suitable to our precision and fast tuning purpose yet easy to implement with widely tunable lasers. Although a multiplier phase detector (frequency mixer) could potentially produce lower phase noise (see, for example [19],), its narrow phase error range (< π) makes it impractical to dynamically phase lock a laser with a frequency noise floor as high as the DS-DBR laser. In contrast, the PFD features not only the widest phase error range (4 π), but also frequency detection when the PLL has not yet acquired lock. Despite the relative high frequency noise floor of the DS-DBR laser and the narrow PLL bandwidth, our OPLL allows the phase-lock to be acquired rapidly and retained robustly without undesirable cycle slips.

It would have been simpler to use the offset sideband-locking technique [20] to achieve the same laser tuning, without requiring the master laser and the OPLL. In this scheme, one sideband of the laser generated from phase modulation is locked to an absolute frequency reference (i.e., a gas absorption line) and the carrier is used as the laser output. The fast laser frequency tuning can then be achieved by rapidly changing the RF of the phase modulation driver (from 0.5 to 20 GHz in every 100 μs). However, such a fast tunable RF source is not available commercially.

The frequency-stepped pulse train can also be generated by combining multiple statically-locked slave lasers as demonstrated in [14]. The design presented here simplifies the system architecture and eliminates the undesirable optical crosstalk among different wavelength channels. This will improve reliability and performance, and reduces the size, mass, power consumption, and cost of the seed laser.

4.2 Tuning speed and range

Since the tuning speed already exceeded our requirements during the initial setup, no further attempt has been made to improve the tuning speed. The abrupt stepping of the target $Sign{\cdot}N{\cdot}f_R$ resulted in a momentary loss of lock and lengthened the lock acquisition time, particularly for the biggest frequency jump (~31 GHz step). The switching time can be shortened by optimizing the feed-forward signal and the loop parameters. For example, one can program the FPGA to synchronously ramp the target $Sign{\cdot}N{\cdot}f_R$ and the feed-forward signal. The dynamic OPLL technique should allow fast quasi-continuous frequency tuning within the ~40 GHz phase section tuning range anywhere in the C- or L-band. For small frequency steps, the tuning time can be shortened to ~1 μs per step.

#167248 - $15.00 USD Received 23 Apr 2012; revised 31 May 2012; accepted 1 Jun 2012; published 12 Jun 2012

So far we have demonstrated the fast tuning within the ~40 GHz range attainable through the phase section alone, which was matched by the 20 GHz PIN-TIA and divider 1. To switch to a target offset frequency beyond this range, the currents to the front and rear mirror sections, along with the feed-forward signal to the phase section, need to be switched jointly [7, 15]. The same OPLL will then phase-lock the laser to the target through the phase section feedback. Furthermore, a separate optical reference (i.e. a master laser line) must be placed near that target frequency so that the beatnote frequency falls within the electronic bandwidth of the detector. To do this, a comb of sidebands can be generated around the master laser by passing the laser through an external phase modulator. The slave laser can also be phase locked to an optical frequency comb generated from a mode-locked laser (see, for example [21],).

4.3 Other applications

Besides applications for high-precision gas sensing lidars, the present laser tuning technique can also be applied to other applications that require such well-controlled precision fast tuning. The technique can be directly applied to a wind sensing lidar that employs a frequency stepped pulse train (see, for example [22],). It could also improve the precision and speed of spectroscopic measurements in a wide wavelength range, compared to other techniques. For example, precision and fast line-shape measurements as illustrated in Fig. 8(b) become possible. It may have potential applications for fast characterization of optical components such as narrow-band optical filters.

5. Conclusions

We have demonstrated a precision and fast wavelength tuning technique for an L-band DS-DBR laser. The laser was dynamically offset-locked to a frequency-stabilized master laser using a fast-tunable OPLL, enabling precision fast tuning to and from any frequencies within a ~40-GHz tuning range. The offset frequency noise was suppressed to the statically offset-locked level in less than ~40 μs upon each frequency switch, allowing the laser to retain the absolute frequency stability of the master laser. This technique satisfies the stringent requirements for gas sensing lidars as exemplified by ASCENDS and enables other applications that require such precision fast tuning. The precision fast tuning range can potentially be expanded to a much wider range.

Acknowledgments

The authors gratefully acknowledge Dr. G. Yang of NASA Goddard for fruitful discussions and his help with RF electronics. They are also indebted to Drs. S. Chandani and P. Mitchell of Oclaro Inc. for their technical support on the DS-DBR lasers, and Dr. J. B. Abshire and other members of the NASA Goddard CO_2 Sounder team for their support. In addition, thanks are due to Dr. Jeffrey Livas of NASA Goddard for his excellent comments on the manuscript. This work was supported by the NASA Earth Science Technology Office Instrument Incubator Program and the NASA Goddard Internal Research and Development Program.

#167248 - $15.00 USD Received 23 Apr 2012; revised 31 May 2012; accepted 1 Jun 2012; published 12 Jun 2012